

Complete Next-to-Leading-Order Corrections to J/ψ Photoproduction in Nonrelativistic Quantum Chromodynamics

Mathias Butenschön and Bernd A. Kniehl

II. Institut für Theoretische Physik, Universität Hamburg, Luruper Chaussee 149, 22761 Hamburg, Germany

(Received 15 September 2009; published 18 February 2010)

We calculate the cross section of inclusive direct J/ψ photoproduction at next-to-leading order within the factorization formalism of nonrelativistic quantum chromodynamics for the first time including the full relativistic corrections due to the intermediate $^1S_0^{[8]}$, $^3S_1^{[8]}$, and $^3P_J^{[8]}$ color-octet states. A comparison of our results to recent H1 data suggests that the color-octet mechanism is indeed realized in J/ψ photoproduction, although the predictivity of our results still suffers from uncertainties in the color-octet long-distance matrix elements.

DOI: 10.1103/PhysRevLett.104.072001

PACS numbers: 12.38.Bx, 13.60.Hb, 13.60.Le, 14.40.Pq

The factorization formalism of nonrelativistic quantum chromodynamics (NRQCD) [1] provides a consistent theoretical framework for the description of heavy-quarkonium production and decay, which is known to hold through two loops [2]. This implies a separation of process-dependent short-distance coefficients to be calculated perturbatively as expansions in the strong-coupling constant α_s from supposedly universal long-distance matrix elements (LDMEs) to be extracted from experiment. The relative importance of the latter can be estimated by means of velocity scaling rules; i.e., the LDMEs are predicted to scale with a definite power of the heavy-quark (Q) velocity v in the limit $v \ll 1$. In this way, the theoretical predictions are organized as double expansions in α_s and v . A crucial feature of this formalism is that it takes into account the complete structure of the $Q\bar{Q}$ Fock space, which is spanned by the states $n = 2S+1 L_J^{[a]}$ with definite spin S , orbital angular momentum L , total angular momentum J , and color multiplicity $a = 1, 8$. In particular, this formalism predicts the existence of color-octet (CO) processes in nature. This means that $Q\bar{Q}$ pairs are produced at short distances in CO states and subsequently evolve into physical color-singlet (CS) quarkonia by the nonperturbative emission of soft gluons. In the limit $v \rightarrow 0$, the traditional CS model (CSM) is recovered in the case of S -wave quarkonia. In the case of J/ψ production, the CSM prediction is based just on the $^3S_1^{[1]}$ CS state, while the leading relativistic corrections, of relative order $\mathcal{O}(v^4)$, are built up by the $^1S_0^{[8]}$, $^3S_1^{[8]}$, and $^3P_J^{[8]}$ ($J = 0, 1, 2$) CO states.

Fifteen years after the introduction of the NRQCD factorization formalism [1], the existence of CO processes and the universality of the LDMEs are still at issue and far from proven, despite an impressive series of experimental and theoretical endeavors. The greatest success of NRQCD was that it was able to explain the J/ψ hadroproduction yield at the Fermilab Tevatron [3], while the CSM prediction lies orders of magnitudes below the data, even if the latter is evaluated at next-to-leading order (NLO) or beyond [4,5]. Also in the case of J/ψ photoproduction at

DESY HERA, the CSM cross section significantly falls short of the data, as demonstrated by a recent NLO analysis [6] using up-to-date input parameters and standard scale choices, leaving room for CO contributions [7]. Similarly, the J/ψ yields measured in electroproduction at HERA and in two-photon collisions at CERN LEP2 were shown [8,9] to favor the presence of CO processes. As for J/ψ polarization in hadroproduction, neither the leading-order (LO) NRQCD prediction [10] nor the NLO CSM one [5] leads to an adequate description of the Tevatron data. The situation is quite similar for the polarization in photoproduction at HERA [6].

In order to convincingly establish the CO mechanism and the LDME universality, it is an urgent task to complete the NLO description of J/ψ hadro- [4,5,11] and photoproduction [6,12], regarding both J/ψ yield [4,12] and polarization [5,6,11], by including the full CO contributions at NLO. While the NLO contributions due to the $^1S_0^{[8]}$ and $^3S_1^{[8]}$ CO states may be obtained [11] using standard techniques, familiar from earliest NLO CSM calculations [12], the NLO treatment of $^3P_J^{[8]}$ states in $2 \rightarrow 2$ processes requires a more advanced technology, which has been lacking so far. In fact, the $^3P_J^{[8]}$ contributions represent the missing links in all of those previous NLO analyses [4–6,11,12], and there is no reason at all to expect them to be insignificant. Specifically, their calculation is far more intricate because the application of the $^3P_J^{[8]}$ projection operators to the short-distance scattering amplitudes produces particularly lengthy expressions involving complicated tensor loop integrals and exhibiting an entangled pattern of infrared (ir) singularities. This technical bottleneck, which has prevented essential progress in the global test of NRQCD factorization for the past 15 years, is overcome here for the first time. So far, only two complete NLO analyses of heavy-quarkonium production in high-energy collisions involving CO states have been performed: the total cross section of hadroproduction [13] and the inclusive cross section at finite transverse momentum p_T in two-photon collisions [14]. However, the former

case corresponds to a $2 \rightarrow 1$ process, which enormously simplifies the calculation, and the latter case does not involve virtual corrections in P -wave channels.

In direct photoproduction, a quasireal photon γ that is radiated off the incoming electron e interacts with a parton i stemming from the incoming proton p . Invoking the Weizsäcker-Williams approximation and the factorization theorems of the QCD parton model and NRQCD [1], the inclusive J/ψ photoproduction cross section is evaluated from

$$d\sigma(ep \rightarrow J/\psi + X) = \sum_{i,n} \int dx dy f_{\gamma/e}(x) f_{i/p}(y) \langle \mathcal{O}^{J/\psi}[n] \rangle \times d\sigma(\gamma i \rightarrow c\bar{c}[n] + X), \quad (1)$$

where $f_{\gamma/e}(x)$ is the photon flux function, $f_{i/p}(y)$ are the parton distribution functions (PDFs) of the proton, $\langle \mathcal{O}^{J/\psi}[n] \rangle$ are the LDMEs, and $d\sigma(\gamma i \rightarrow c\bar{c}[n] + X)$ are the partonic cross sections. Working in the fixed-flavor-number scheme, i runs over the gluon g and the light quarks $q = u, d, s$, and antiquarks \bar{q} .

The Feynman amplitudes of $\gamma i \rightarrow c\bar{c}[n] + X$ are calculated by the application of appropriate spin and color projectors onto the usual Feynman amplitudes for open $c\bar{c}$ production [13]. Example Feynman diagrams for partonic LO subprocesses as well as virtual- and real-correction diagrams are shown in Fig. 1. Important properties of these projections are that the relative momentum q between the c and \bar{c} quarks has to be set to zero, in the case of P -wave states after taking the derivative with respect to q .

We checked analytically that all appearing singularities cancel. As for the ultraviolet singularities, we renormalize the charm-quark mass and the wave functions of the external particles according to the on-shell scheme and the strong-coupling constant according to the modified minimal-subtraction scheme. Figure 2 displays an overview of the ir singularity structure. In the case of the $^3S_1^{[1]}$, $^1S_0^{[8]}$, and $^3S_1^{[8]}$ states, the soft and collinear singularities of the real corrections are canceled as usual by complementary contributions stemming from the virtual corrections and by the absorption of universal parts into the proton and photon PDFs, the latter entering via resolved photoproduction. In the case of the $^3P_J^{[8]}$ states, the soft-singularity structure is more complex. The reason is the following:

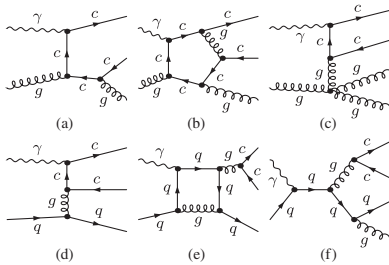


FIG. 1. Sample diagrams contributing at LO [(a) and (d)] and to the virtual [(b) and (e)] and real [(c) and (f)] NLO corrections.

in the soft limit, the real-correction amplitudes factorize into LO amplitudes and so-called eikonal factors. Taking the derivative with respect to q and squaring the amplitudes then leads to additional soft #2 and soft #3 terms because the derivative has to be taken of the eikonal factors as well. The soft #3 terms are proportional to a linear combination of the short-distance cross sections to produce the $^3S_1^{[1]}$ and $^3S_1^{[8]}$ states. They are canceled against ir singularities stemming from radiative corrections to the $\langle \mathcal{O}^{J/\psi}(^3S_1^{[1]}) \rangle$ and $\langle \mathcal{O}^{J/\psi}(^3S_1^{[8]}) \rangle$ LDMEs. The soft #2 terms do not factorize to LO cross sections. They also cancel against virtual-correction contributions as the usual soft #1 terms.

Apart from the analytical cancellation of all occurring singularities, our calculation passes a number of further nontrivial checks. We implemented two independent methods for the reduction of the tensor loop integrals, which yielded identical results. As for the real corrections, the numerical evaluation of our expressions for the squared matrix elements agrees with numerical output generated using the program package MADONIA [15], well within the numerical uncertainty of the latter. We verified that our results are stable with respect to variations of the phase space slicing parameters introduced as a demarcation between the soft and/or collinear regions from the rest of the three-particle phase space. Finally, we could nicely reproduce the NLO CSM results of Ref. [12] after adopting the inputs chosen therein. For space limitation, we refrain from presenting here more technical details but refer the interested reader to a forthcoming publication.

We now describe our theoretical input and the kinematic conditions for our numerical analysis. We set $m_c = m_{J/\psi}/2$, adopt the values of $m_{J/\psi}$, m_e , and α from Ref. [16], and use the one-loop (two-loop) formula for $\alpha_s^{(n_f)}(\mu)$, with $n_f = 3$ active quark flavors, at LO (NLO). As for the proton PDFs, we use set CTEQ6L1 (CTEQ6M) [17] at LO (NLO), which comes with an asymptotic scale parameter of $\Lambda_{\text{QCD}}^{(4)} = 215 \text{ MeV}$ (326 MeV), so that $\Lambda_{\text{QCD}}^{(3)} = 249 \text{ MeV}$ (389 MeV). We evaluate the photon flux function using Eq. (5) of Ref. [18] with the cutoff $Q_{\text{max}}^2 = 2 \text{ GeV}^2$ [19,20] on the photon virtuality. Our default choices for the renormalization, factorization, and NRQCD scales are $\mu_r = \mu_f = m_T$ and $\mu_\Lambda = m_c$, respectively, where $m_T = \sqrt{p_T^2 + 4m_c^2}$ is the J/ψ transverse

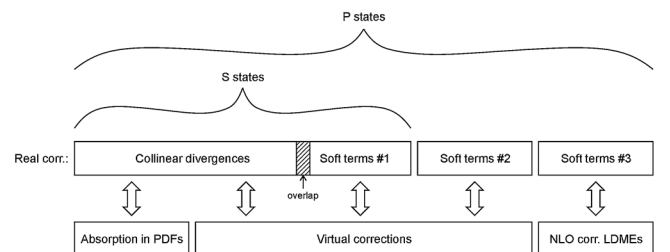


FIG. 2. Overview of the ir singularity structure.

mass. We adopt the LDMEs from Ref. [21], which were fitted to Tevatron I data using the CTEQ4 PDFs, because, besides the usual LO set, they also comprise a higher-order-improved set determined by approximately taking into account dominant higher-order effects due to multiple-gluon radiation in inclusive J/ψ hadroproduction, which had been found to be substantial by a Monte Carlo study [22]. This observation is in line with the sizable NLO corrections recently found in Refs. [4,5,11], still excluding the $^3P_J^{[8]}$ channels at NLO. Of course, LDME fits to more recent Tevatron data are available, but their goodness is clearly limited by the present theoretical uncertainties in the short-distance cross sections, preventing the increase in experimental precision gained since the analysis of Ref. [21] from actually being beneficial. Apart from that, the central values of the J/ψ LDMEs have only moderately changed, as may be seen by comparing the LO results of Ref. [21] with those recently obtained [23] by fitting Tevatron II data using the CTEQ6L1 PDFs [17]. Because the p_T distributions of the $^1S_0^{[8]}$ and $^3P_J^{[8]}$ contributions to J/ψ hadroproduction exhibit very similar shapes, fits usually only constrain the linear combination

$$M_r^{J/\psi} = \langle \mathcal{O}^{J/\psi}(^1S_0^{[8]}) \rangle + \frac{r}{m_c^2} \langle \mathcal{O}^{J/\psi}(^3P_0^{[8]}) \rangle, \quad (2)$$

with an r value of about 3.5 [21,23]. As in Ref. [14], we take the democratic choice $\langle \mathcal{O}^{J/\psi}(^1S_0^{[8]}) \rangle = (r/m_c^2) \times \langle \mathcal{O}^{J/\psi}(^3P_0^{[8]}) \rangle = M_r^{J/\psi}/2$ as our default.

Recently, the H1 Collaboration presented new data on inclusive J/ψ photoproduction taken in collisions of 27.6 GeV electrons or positrons on 920 GeV protons in the HERA II laboratory frame [20]. They nicely agree with their previous measurement at HERA I [19]. These data come as singly differential cross sections in p_T^2 , $W = \sqrt{(p_\gamma + p_p)^2}$, and $z = (p_{J/\psi} \cdot p_p)/(p_\gamma \cdot p_p)$, in each case with certain acceptance cuts on the other two variables. Here, p_γ , p_p , and $p_{J/\psi}$ are the photon, proton, and J/ψ four-momenta, respectively. In the comparisons below, we impose the same kinematic conditions on our theoretical predictions.

We start our numerical analysis by estimating the theoretical uncertainties. The dependences on the unphysical scales μ_r and μ_f are investigated in full NRQCD at LO and NLO for the typical case of $d\sigma(ep \rightarrow J/\psi + X)/dp_T^2$ at $p_T^2 = 20 \text{ GeV}^2$ in Fig. 3. Contrary to naive expectations, the scale dependence is not reduced when passing from LO to NLO. Detailed investigation reveals that this behavior may be ascribed to the fact that the new coefficient of $\alpha_s^3(\mu_r)$ is greatly dominated by the part that does not carry logarithmic dependence on μ_r or μ_f , mainly arising from the gluon-induced $^1S_0^{[8]}$ and $^3P_0^{[8]}$ channels, while the complementary part still formally warrants renormalization group invariance up to terms beyond NLO. As for the dependence on m_c , a reduction of m_c from $m_{J/\psi}/2 \approx$

1.55 GeV to 1.4 GeV typically entails a rise in cross section by about 50%. The freedom in sharing $M_r^{J/\psi}$ of Eq. (2) between $\langle \mathcal{O}^{J/\psi}(^1S_0^{[8]}) \rangle$ and $(r/m_c^2) \langle \mathcal{O}^{J/\psi}(^3P_0^{[8]}) \rangle$ typically creates an uncertainty of about 10%. The bulk of the theoretical uncertainty is actually due to the lack of knowledge of the complete NLO corrections to the cross section of inclusive J/ψ hadroproduction, which is instrumental for a reliable NLO fit of the CO LDMEs to the Tevatron data. As explained above, these corrections are expected to be dominated by positive and sizable contributions from real QCD bremsstrahlung [4,5,11,22], leading to a significant reduction of the CO LDMEs [21]. At present, the theoretical uncertainty in inclusive J/ψ photoproduction from this source may be conservatively estimated by comparing the full NRQCD evaluations using the LO and higher-order-improved LDME sets of Ref. [21] with the understanding that the former is bound to overshoot a future evaluation with a genuine NLO set. This kind of uncertainty is indicated in the remaining figures by shaded (yellow) bands, whose upper margins (solid lines) refer to the LO set.

The H1 measurements [19,20] of the p_T^2 , W , and z distributions of inclusive J/ψ photoproduction are compared with our new NLO predictions in full NRQCD in Figs. 4(a)–4(c), respectively. For comparison, the default predictions at LO (dashed lines) as well as those of the CSM at NLO (dot-dashed lines) and LO (dotted lines) are also shown. Notice that the experimental data are contaminated by the feed-down from heavier charmonia, mainly due to $\psi' \rightarrow J/\psi + X$, which yields an estimated enhancement by about 15% [12]. Furthermore, our predictions do not include resolved photoproduction, which contributes appreciably only at $z \lesssim 0.3$ [21], and diffractive production, which is confined to the quasielastic domain at $z \approx 1$ and $p_T \approx 0$. These contributions are efficiently suppressed by the cut $0.3 < z < 0.9$ in Figs. 4(a) and 4(b), so that our comparisons are indeed meaningful. We observe that the NLO corrections enhance the NRQCD cross section by up to 115% in the kinematic range con-

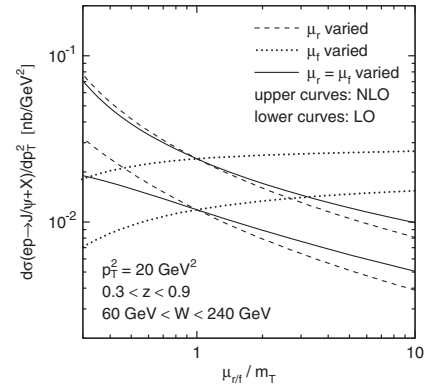


FIG. 3. Separate and joint dependences of $d\sigma(ep \rightarrow J/\psi + X)/dp_T^2$ at $p_T^2 = 20 \text{ GeV}^2$ in full NRQCD at LO and NLO on μ_r and μ_f .

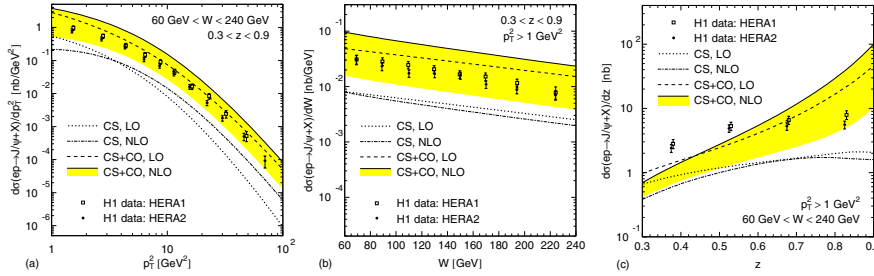


FIG. 4 (color online). (a) p_T^2 , (b) W , and (c) z distributions of inclusive J/ψ photoproduction at LO and NLO in the CSM and full NRQCD in comparison with H1 data [19,20]. The shaded (yellow) bands indicate the theoretical uncertainty due to the CO LDMEs.

sidered, except for $z \lesssim 0.45$, where they are negative. As may be seen from Fig. 4(c), the familiar growth of the LO NRQCD prediction in the upper end point region, leading to a breakdown at $z = 1$, is further enhanced at NLO. The solution to this problem clearly lies beyond the fixed-order treatment and may be found in soft collinear effective theory [24]. The experimental data are nicely gathered in the central region of the error bands, except for the two low- z points in Fig. 4(c), which overshoot the NLO NRQCD prediction. However, this apparent disagreement is expected to fade away once the NLO-corrected NRQCD contribution due to resolved photoproduction is included. In fact, the above considerations concerning the large size of the NLO corrections to hadroproduction directly carry over to resolved photoproduction, which proceeds through the same partonic subprocesses. On the other hand, the default CSM predictions significantly undershoot the experimental data by typically a factor of 4, which has already been observed in Ref. [6]. Except for $p_T^2 \gtrsim 4 \text{ GeV}^2$, the situation is even deteriorated by the inclusion of the NLO corrections.

Despite the caveat concerning our limited knowledge of the CO LDMEs at NLO, we conclude that the H1 data [19,20] show clear evidence of the existence of CO processes in nature, as predicted by NRQCD, supporting the conclusions previously reached for hadroproduction at the Tevatron [3] and two-photon collisions at LEP2 [9]. In order to further substantiate this argument, it is indispensable to determine the relevant CO LDMEs with NLO precision. Since the tightest constraints have so far come from the Tevatron and soon will from the CERN LHC, the most urgent next step is to complete the NLO analysis of inclusive J/ψ hadroproduction in NRQCD by also treating the $^3P_J^{[8]}$ channels at NLO. This goal is greatly facilitated by the technical advancement achieved in the present analysis.

We thank L. Mihaila and J. Soto for useful discussions, and M. Steder for help with the comparison to H1 data [20]. This work was supported in part by BMBF Grant No. 05H09GUE, DFG Grant No. KN 365/6-1, and HGF Grant No. HA 101.

[1] G. T. Bodwin, E. Braaten, and G. P. Lepage, Phys. Rev. D **51**, 1125 (1995); **55**, 5853(E) (1997).

[2] G. C. Nayak, J. W. Qiu, and G. Sterman, Phys. Rev. D **72**, 114012 (2005); **74**, 074007 (2006).
 [3] P. L. Cho and A. K. Leibovich, Phys. Rev. D **53**, 150 (1996); **53**, 6203 (1996).
 [4] J. Campbell, F. Maltoni, and F. Tramontano, Phys. Rev. Lett. **98**, 252002 (2007); P. Artoisenet, J. P. Lansberg, and F. Maltoni, Phys. Lett. B **653**, 60 (2007); P. Artoisenet, AIP Conf. Proc. **1038**, 55 (2008).
 [5] B. Gong and J.-X. Wang, Phys. Rev. Lett. **100**, 232001 (2008).
 [6] P. Artoisenet, J. Campbell, F. Maltoni, and F. Tramontano, Phys. Rev. Lett. **102**, 142001 (2009); C.-H. Chang, R. Li, and J.-X. Wang, Phys. Rev. D **80**, 034020 (2009).
 [7] M. Cacciari and M. Krämer, Phys. Rev. Lett. **76**, 4128 (1996); P. Ko, J. Lee, and H. S. Song, Phys. Rev. D **54**, 4312 (1996); **60**, 119902(E) (1999).
 [8] B. A. Kniehl and L. Zwierner, Nucl. Phys. **B621**, 337 (2002).
 [9] M. Klasen, B. A. Kniehl, L. N. Mihaila, and M. Steinhauser, Phys. Rev. Lett. **89**, 032001 (2002).
 [10] E. Braaten, B. A. Kniehl, and J. Lee, Phys. Rev. D **62**, 094005 (2000); B. A. Kniehl and J. Lee, *ibid.* **62**, 114027 (2000).
 [11] B. Gong, X. Q. Li, and J.-X. Wang, Phys. Lett. B **673**, 197 (2009).
 [12] M. Krämer, J. Zunft, J. Steegborn, and P. M. Zerwas, Phys. Lett. B **348**, 657 (1995); M. Krämer, Nucl. Phys. **B459**, 3 (1996).
 [13] A. Petrelli, M. Cacciari, M. Greco, F. Maltoni, and M. L. Mangano, Nucl. Phys. **B514**, 245 (1998).
 [14] M. Klasen, B. A. Kniehl, L. N. Mihaila, and M. Steinhauser, Nucl. Phys. **B713**, 487 (2005); Phys. Rev. D **71**, 014016 (2005).
 [15] P. Artoisenet, F. Maltoni, and T. Stelzer, J. High Energy Phys. **02** (2008) 102.
 [16] C. Amsler *et al.* (Particle Data Group), Phys. Lett. B **667**, 1 (2008).
 [17] J. Pumplin *et al.* (CTEQ Collaboration), J. High Energy Phys. **07** (2002) 012.
 [18] B. A. Kniehl, G. Kramer, and M. Spira, Z. Phys. C **76**, 689 (1997).
 [19] C. Adloff *et al.* (H1 Collaboration), Eur. Phys. J. C **25**, 25 (2002).
 [20] F. D. Aaron *et al.* (H1 Collaboration), DESY 09-225, arXiv:1002.0234.
 [21] B. A. Kniehl and G. Kramer, Eur. Phys. J. C **6**, 493 (1999).
 [22] B. Cano-Coloma and M. A. Sanchis-Lozano, Nucl. Phys. **B508**, 753 (1997).
 [23] B. A. Kniehl and C. P. Palisoc, Eur. Phys. J. C **48**, 451 (2006).
 [24] S. Fleming, A. K. Leibovich, and T. Mehen, Phys. Rev. D **74**, 114004 (2006).